Langmuir Article

pubs.acs.org/Langmuir

Structure of the Sodium Dodecyl Sulfate Surfactant on a Solid Surface in Different NaCl Solutions

Hector Domínguez*

Instituto de Investigaciones en Materiales, Universidad Nacional Autónoma de México, UNAM, México DF 04510, Mexico

Received February 27, 2009. Revised Manuscript Received June 4, 2009

Studies of molecular dynamics simulations of sodium dodecyl sulfate (SDS) molecules adsorbed on a graphite surface in different salt (NaCl)/water solutions were conducted. The results showed the formation of hemicylindrical aggregates, at different salt concentrations, in agreement with atomic force microscopy (AFM) results. However, the hemicylinders exhibited different structures as the salt concentration was increased. At low concentrations, the internal structure of the hemicylinder formed well-defined SDS layers, parallel to the surface. However, when the amount of salt was increased, the top layer became less pronounced until it disappeared at the highest concentration. Density profiles of the SDS headgroups were also analyzed, and those profiles were found to become sharper as the NaCl concentration increased. The phenomenon was investigated in terms of how the aggregates wet the solid surface.

1. Introduction

Surfactant adsorption at interfaces has been investigated not only for its scientific interest but also for its applicability in industrial processes such as detergency, lubrication, corrosion, colloid stabilization, etc. It can also help us to better understand processes in electrochemistry and electrode surfaces areas, among others.[1] Several experiments aimed at studying the behavior of surfactants at liquid−air and liquid−liquid interfaces have been conducted;[2−6] however, the self-assembly of surfactants in the presence of a solid surface has been investigated less. At present, it is well-known that surfactant molecules self-aggregate into spheres, cylinders, and bilayers in bulk solutions. However, how aggregation is modified by the presence of solid surfaces is not yet clear. Several experiments suggest that most of the aggregates observed in bulk solutions can also appear at solid−liquid interfaces.[1,7−10] However, the nature, structure, and shape of those aggregates show different features due to the extra solid−surfactant interaction. Therefore, over the past few years, several experimental methods have been widely employed to study aggregation of surfactants at solid plates.[11−17] Among all those experimental techniques, atomic force microscopy (AFM) has been particularly useful in studying self-assembly of surfactants on solid surfaces.[1,10,18−20] In particular, AFM results show that the sodium dodecyl sulfate (SDS) surfactant forms hemicylinders on a graphite surface.[21] Another surfactant such as C_{14}TAB forms hemicylinders on hydrophobic substrates, full cylinders on mica, and spheres on amorphous silica.[18]

In fact, there is a general agreement that surfactants on hydrophobic surfaces (e.g., graphite) self-organize in hemicylinders since the substrates interact primarily with the tail groups through van der Waals forces.[10] However, hydrophilic substrates interact primarily with the surfactant headgroups giving rise to different aggregates on the surfaces. Different studies have been conducted to investigate the self-assembly as a function of the surfactant chain length[9] and as a function of the polar headgroup.[19]

On the other hand, over the past few years, computer simulations have become an important tool for the study of such complex interfacial systems. From computer experiments, it is possible to extract information about dynamical, thermodynamical, and structural properties of interfacial systems at the molecular level, which sometimes are not easy to obtain from real experiments. Therefore, simulations from fully atomistic[22−28]

*E-mail: hectordc@servidor.unam.mx.

(1) Jaschke, M.; Butt, H.-J.; Gaub, H. E.; Manne, S. *Langmuir* **1997**, *13*, 1381.
(2) Saccani, J.; Castano, S.; Beaurain, F.; Laguerre, M.; Desbat, B. *Langmuir* **2004**, *20*, 9190.
(3) Conboy, J. C.; Messmer, M. C.; Richmond, G. *Langmuir* **1998**, *14*, 6722.
(4) Zhang, Z. H.; Tsuyumoto, I.; Kitamori, T.; Sawada, T. *J. Phys. Chem. B* **1998**, *102*, 10284.
(5) Lyttle, D. J.; Lu, J. R.; Su, T. J.; Thomas, R. K.; Penfold, J. *Langmuir* **1995**, *11*, 1001.
(6) Lu, J. R.; Hromadova, M.; Simister, E. A.; Thomas, R. K.; Penfold, J. *J. Phys. Chem.* **1994**, *98*, 11519.
(7) Grant, L. M.; Tiberg, F.; Ducker, W. A. *J. Phys. Chem. B* **1998**, *102*, 4288.
(8) Ducker, W. A.; Wanless, E. J. *Langmuir* **1999**, *15*, 160.
(9) Ducker, W. A.; Grant, L. M. *J. Phys. Chem.* **1996**, *100*, 11507.
(10) Manne, S.; Cleveland, J. P.; Gaub, H. E.; Stucky, G. D.; Hansma, P. K. *Langmuir* **1994**, *10*, 4409.
(11) Király, Z.; Findenegg, G. H. *J. Phys. Chem. B* **1998**, *102*, 1203.
(12) Penfold, J.; Staples, E. J.; Tucker, I.; Thompson, L. J. *Langmuir* **1997**, *13*, 16638.
(13) Luciani, L.; Denoyel, R. *J. Colloid Interface Sci.* **1997**, *188*, 7580.
(14) McDermott, D. C.; McCarney, J.; Thomas, R. K.; Rennie, A. R. *J. Colloid Interface Sci.* **1994**, *162*, 304.
(15) Pashley, R. M.; McGuiggan, P. M.; Horn, R. G.; Ninham, B. W. *J. Colloid Interface Sci.* **1988**, *126*, 569.
(16) Tilberg, F.; Joensson, B.; Tang, J.; Lindmann, B. *Langmuir* **1994**, *10*, 2294.
(17) Levitz, P.; Van Damme, H. *J. Phys. Chem.* **1986**, *90*, 1302.
(18) Manne, S.; Gaub, H. E. *Science* **1995**, *270*, 1480.
(19) Patrick, H. N.; Warr, G. G.; Manne, S.; Aksay, I. A. *Langmuir* **1997**, *13*, 4349.
(20) Ducker, W. A.; Wanless, E. J. *Langmuir* **1996**, *12*, 5915.
(21) Wanless, E. J.; Ducker, W. A. *J. Phys. Chem.* **1996**, *100*, 3207.
(22) krishnan, M.; Balasubramanian, S. *Phys. Chem. Chem. Phys.* **2005**, *7*, 2044.
(23) Bandyopadhyay, S.; Shelley, J. C.; Tarek, M.; Moore, P. B.; Klein, M. L. *J. Phys. Chem. B* **1998**, *102*, 6318.
(24) Werder, T.; Walther, J. H.; Jaffe, R. L.; Halicioglu, T.; Koumoutsakos, P. *J. Phys. Chem. B* **2003**, *107*, 1345.
(25) Zheng, F.; Zhang, X.; Wang, W.; Dong, W. *Langmuir* **2006**, *22*, 11214.
(26) Shah, K.; Chiu, P.; Sinnott, S. B. *J. Colloid Interface Sci.* **2006**, *296*, 342.
(27) Sammalkorpi, M.; Panagiotopoulos, A. Z.; Haataja, M. *J. Phys. Chem. B* **2008**, *112*, 2915.
(28) Sammalkorpi, M.; Panagiotopoulos, A. Z.; Haataja, M. *J. Phys. Chem. B* **2008**, *112*, 12954.

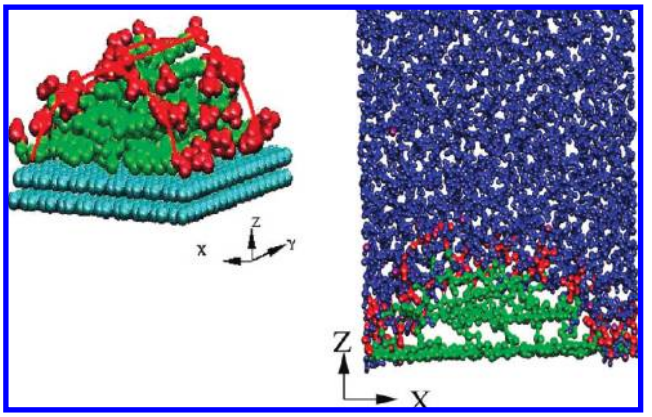

Figure 1. Three-dimensional snapshot (left; the lines in the picture are just to guide the form of the hemicylinder) and $X-Z$ projection (right) of the SDS surfactant on a graphite surface at a NaCl concentration of 0.0166 cc.

to coarse-grain models[29−32] have been conducted in this direction. For instance, some groups have observed how surfactants with short tails form monolayers and surfactants with long tails form hemicylinders on a graphite surface,[29] whereas other groups have investigated structures of binary mixtures (SDS and dodecane) on solid surfaces.[27]

In a previous work, aggregation of SDS molecules on a graphite surface was investigated, and the shape of the aggregates was found to depend on SDS concentration.[33] In this work, the structure of the aggregates on a graphite substrate was studied as a function of a salt (NaCl) in solution. For this particular system, experimental results show that the shape of the aggregates did not change significantly with salt concentration, although the aggregates moved close together as the NaCl concentration increased.[21]

2. Computational Method and Model

Simulations were conducted for anionic sodium dodecyl sulfate (SDS) molecules by using an atomistic model of a hydrocarbon chain of 12 united carbon atoms attached to a headgroup, SO_4^-. The simulation parameters for the SDS were the same as described in previous works.[33,34] For water, the SPC model was used, and for the graphite surface, two layers were constructed by using an atomistic model.

The initial configuration was prepared from a monolayer of 36 surfactant molecules in the all-trans configuration (placed close to the graphite) with the SDS headgroups initially pointing toward the solid surface with X and Y dimensions of 40.249 Å. Then, 2416 water molecules and 36 sodium cations (Na^+) were added to the system. The usual periodic boundary conditions were imposed in the simulation box. However, the box length in the Z-direction was chosen so that it was long enough ($Z = 150$ Å) to prevent the formation of a second water−solid interface. In this way, a liquid−vapor interface was formed far from the liquid−solid interface.

Since the interest in this work was to study the effects of salt on the structure of the aggregates, different NaCl salt concentrations were added to the system. The salt was included by adding randomly Na^+ (besides the Na^+ ions from the SDS molecules) and Cl^- particles to the water solution.

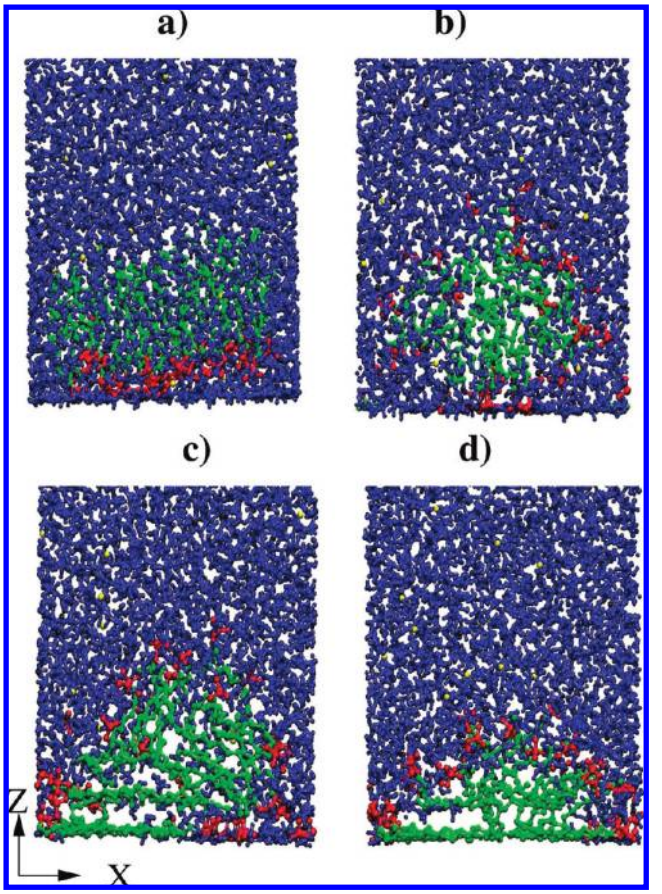

Figure 2. Snapshots of the SDS surfactant, for a salt concentration of 0.0166 cc, on a graphite surface at different simulation times: (a) 50 ps, (b) 2 ns, (c) 5 ns, and (d) 7 ns.

All simulations were conducted in the NVT ensemble using the DL-POLY package[35] with a time step of 0.002 ps. The temperature was 300 K, using the Hoover-Nose thermostat with a relaxation time of 0.2 ps.[36] The long-range electrostatic interactions were handled with the particle mesh Ewald method with a precision of 10^{-4}, and the van der Waals interactions were cut off at 10 Å. Finally, simulations were conducted for up to 17 ns, where the last 4 ns was used for data analysis. Configurational energy was monitored as a function of time as a parameter to determine when the system reached equilibrium.

3. Results

In this section, the results of the simulations for the SDS surfactant adsorbed on a graphite surface at different salt concentrations are presented. The first simulation was conducted without NaCl, and then four other simulations at different concentrations were conducted: 0.0166 cc (20 ion pairs), 0.0331 cc (40 ions pairs), 0.0497 cc (60 ions pairs), and 0.0662 cc (80 ion pairs). The NaCl concentration was defined as the total number of ion pairs (Na and Cl) divided by the total number of water molecules (i.e., the ratio of NaCl to H_2O molecules).

3.1. Surfactant Structure at the Interface. The system with 36 SDS molecules at the interface had a surface coverage of 45 $Å^2$/molecule, which is the area per headgroup at the critical micelle

(29) Srinivas, G.; Nielsen, S. O.; Moore, P. B.; Klein, M. L. *J. Am. Chem. Soc.* **2006**, *128*, 848.
(30) Kranenburg, M.; Venturoli, M.; Smit, B. *J. Phys. Chem. B* **2003**, *107*, 11491.
(31) Goetz, R.; Gompper, G.; Lipowsky, R. *Phys. Rev. Lett.* **1999**, *82*, 221.
(32) Shelley, J. C.; Shelley, M.; Reeder, R.; Bandyopadhyay, S.; Klein, M. L. *J. Phys. Chem. B* **2001**, *105*, 4464.
(33) Dominguez, H. *J. Phys. Chem. B* **2007**, *111*, 4054.
(34) Dominguez, H.; Rivera, M. *Langmuir* **2005**, *21*, 7257.
(35) Forester, T. R.; Smith, W. *DL-POLY Package of Molecular Simulation*; CCLRC Daresbury Laboratory: Daresbury, Warrington, England, 1996.
(36) Hoover, W. G. *Phys. Rev. A* **1985**, *31*, 1695.

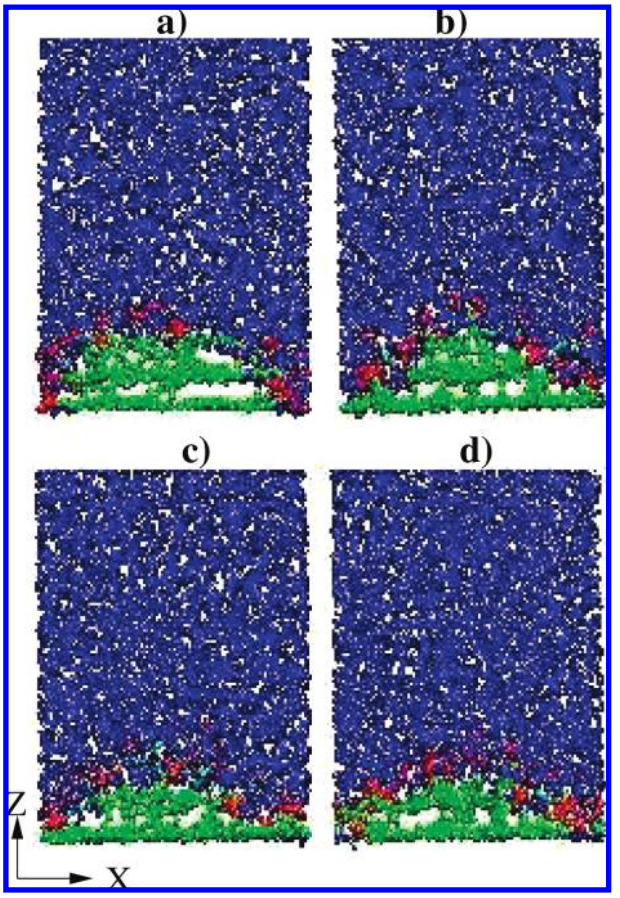

Figure 3. Snapshots of the SDS surfactant on a graphite surface at NaCl concentrations of (a) 0.0166, (b) 0.0331, (c) 0.0497, and (d) 0.0662 cc.

concentration at the water−vapor interface.[37] At this surface coverage, the SDS headgroups next to the surface were rapidly repelled from the graphite surface since there was a strong affinity between the graphite atoms and the carbons in the tails. In all simulations, regardless of the NaCl concentration, the formation of hemicylindrical-like shapes was observed.

It is worth mentioning that we have found hemicylinders that are the structures formed on the surface to be consistent with the term used in experimental findings. However, at this moment, we cannot assume that those shapes were exactly half-cylinders. This point will be discussed later in the paper.

In Figure 1, a three-dimensional snapshot of the aggregate at 0.0166 cc is shown. The axis of the hemicylinder is parallel to the *Y*-axis, whereas a hemicircle in the *X*−*Z* plane is observed.

As mentioned above, the initial configuration started from a monolayer of SDS molecules. However, this structure was changing with time until it formed a hemicylinder, and it kept that structure until the end of the simulation. It is important to note that the hemicylinder was formed at different times depending of the salt concentration; at 0.0 cc, the hemicylinder was formed at ≈9 ns, at 0.0166 cc at ≈7 ns, at 0.0166 cc at ≈6 ns, at 0.0166 cc at ≈5 ns, and at 0.0166 cc at ≈4 ns. Since the total simulation time was 17 ns, the aggregates preserved their hemicylindrical structures for more than 8 ns which suggested that they reached an equilibrium state.

(37) Lu, J. R.; Marroco, A.; Su, T. J.; Thomas, R. K.; Penfold, J. *J. Colloid Interface Sci.* **1993**, *158*, 303.

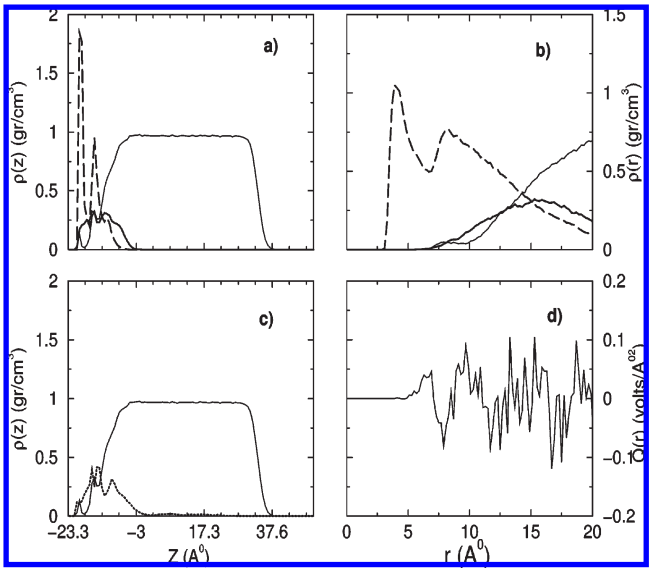

Figure 4. (a and c) *z*-density profiles [$\rho(z)$] without NaCl. Data for water are represented by the light solid line, for SDS headgroups by the dark solid line, and for SDS tails by the dashed line (a). Data for Na^+ ions are represented by the dotted line (c), where the Na^+ profile was scaled by a factor of 10. (b and d) *r*-density profile [$\rho(r)$] and the total charge density profile [$Q(r)$] without NaCl.

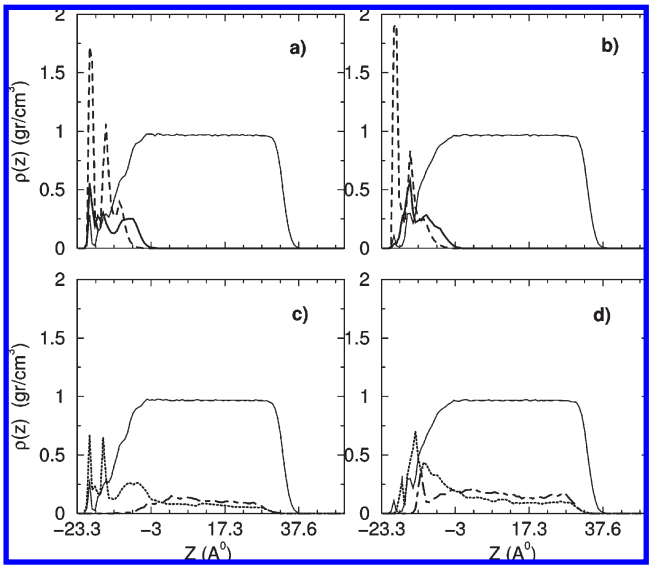

Figure 5. *z*-density profiles [$\rho(z)$] for the SDS molecules on a graphite surface for NaCl concentrations of 0.0166 cc (a and c) and 0.0331 cc (b and d). Data for water are represented by the light solid line, for SDS headgroups by the dark solid line, for SDS tails by the dashed line (a,b), for Na^+ ions by the dotted line, and for Cl^- ions by the dotted−dashed lines (c,d), where the Na^+ and Cl^- profiles were scaled by a factor of 10.

In Figure 2, the evolution of the SDS molecules for a salt concentration of 0.0166 cc at different times is shown (*X*−*Z* plane projection). Here, we can depict that the hemicylinder shape was already formed around 7 ns. In Figure 3, snapshots of the last configuration, projected on the *X*−*Z* plane, for all salt concentrations are shown where the formation of hemicylinders was observed in all cases.

In Figures 4−6, the SDS structure on the graphite surface was investigated in terms of the density profiles of the molecules for all NaCl concentrations. There, the *z*-dependent density profiles

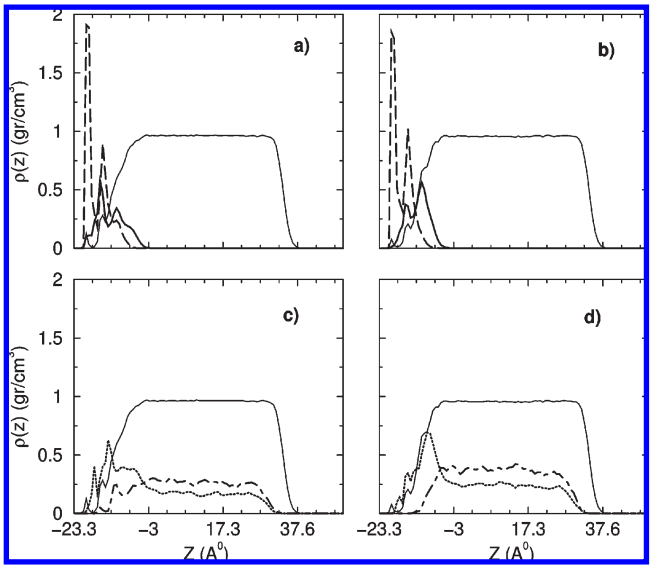

Figure 6. z-density profiles [$\rho(z)$] for the SDS molecules on a graphite surface at NaCl concentrations of 0.0497 cc (a and c) and 0.0662 cc (b and d). The notation is the same as in Figure 5.

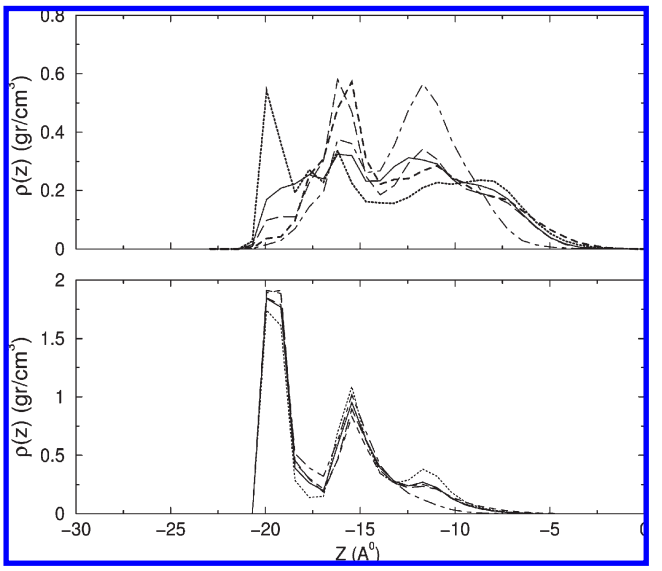

Figure 7. z-density profiles [$\rho(z)$] for the headgroups (top) and tails (bottom) as a function of salt concentration: (—) 0.0, (···) 0.0166, (---) 0.0331, (− − −) 0.0497, and (·−·) 0.0662 cc.

[$\rho(z)$] for the water, the headgroups, the hydrocarbon tails, the Na^+ ions, and the Cl^- ions were shown in the z-direction, i.e., normal to the liquid−solid interface. From those figures, a water−air interface at $Z \approx 30$ Å was observed. Moreover, the density profiles without NaCl were similar to those obtained in our previous work.[33]

From the profiles, it was interesting to note that the SDS tails were adsorbed on the graphite substrate and were arrayed in well-defined layers, parallel to the surface. When a detailed analysis of the systems was conducted, it was noted that the structure of those layers depended on the NaCl concentration. Without NaCl, two peaks which corresponded to two well-defined layers were formed. At the same time, a third small peak indicated the formation of a third layer [at the top of the hemicylinder (see Figure 4a)]. The same trend was observed at salt concentrations of 0.0166 and 0.0331 cc (Figure 5a,b). However, as the salt concentration increased, the third layer became less pronounced until it vanished at the highest concentrations, 0.0497 and 0.0662 cc (Figure 6a,b). In Figure 7, the density profiles for the headgroups and the tails, in two separate plots, as a function of salt concentration are shown. In Figures 1 and 3 are shown the snapshots for all concentrations where it was observed that at low concentrations three layers were developed, whereas at higher concentrations, only two well-defined layers remained. It was also interesting to notice that the headgroup density profiles became sharper as the salt concentration in water increased.

The total length of the tails was measured as the distance from the first to the last carbon in the tails, and average lengths (l) of 11.8, 11.9, 11.6, 11.8, and 11.2 Å for salt concentrations of 0.0, 0.0166, 0.0331, 0.0497, and 0.0662 cc, respectively, were found. If the headgroup length (≈3.0 Å) is added to those values, a rough estimation of the total average SDS length between ≈14.5 and 15.0 Å is obtained. Since the size of the SDS molecule was approximately 17 Å, these results indicated that the tails were not completely straight.

On the other hand, extra information was obtained from the radial density profiles [$\rho(r)$]. Here, r (the radial variable on the $X-Z$ plane) was defined as $r^2 = (x^2 + z^2)$, where the value $r = 0$ was located at the center of the hemicircle which was calculated from the middle point of the distance between the opposite headgroups in the first contact layer with the solid plate.

The results are shown in Figures 4, 8, and 9. From these plots, it was also possible to assume that the shape of the aggregates was hemicylinder-like with the tails located inside and the headgroups pointed outside surrounded by water molecules. By fitting a Gaussian to the headgroup profiles, we estimated the average r-distance of the hemicylinders. By this procedure, values of 15.5, 17.3, 15.9, 16.4, and 15.5 Å (with an error of ±1) for NaCl concentrations of 0.0, 0.0166, 0.0331, 0.0497, and 0.0662 cc, respectively, were found. The data are also given in Table 1. Although these values give us information about the size of the hemicylinders, we have to be careful in associating the data with the radii of the hemicylinders.

With AFM experiments, researchers have found (for the same system of SDS on graphite) aggregates with a height of ∼17 Å.[21] If AFM measures the height of the aggregates on the z-axis (perpendicular to the surface), then, it will be realistic to compare the values with the results obtained from the $\rho(z)$ profiles. Therefore, we calculated the height of the structures by measuring the distance from the first to the last points in the headgroup profiles, and we found a height (l) of ≈17 Å for all NaCl concentrations, which were in good agreement with experimental results. However, this value is smaller than the radius of spherical SDS micelles in bulk, which is 2 nm.[38]

From the structural point of view, hemicylindrical aggregates were obtained in all cases. However, those aggregates could present different characteristics at the surface; i.e., they might wet the surface in different ways. To investigate the wetting on the surface, we conducted a simple contact angle study. The contact angle was calculated as follows; for a given configuration and concentration, a circle was fitted [$(X - X_0)^2 + (Z - Z_0)^2 = R^2$] to the positions of the headgroups (mainly the sulfur atoms) over the $X-Z$ projection. Once the best fitting was obtained, the slope of the curve at the position where the circle hit the graphite plane was calculated. Then, the contact angle was obtained as an average over 10 different configurations. The same procedure was conducted for all concentrations to yield average contact angles of

(38) Zapf, A.; Beck, R.; Platz, G.; Hoffmann, H. *Adv. Colloid Interface Sci.* **2003**, *100*, 349.

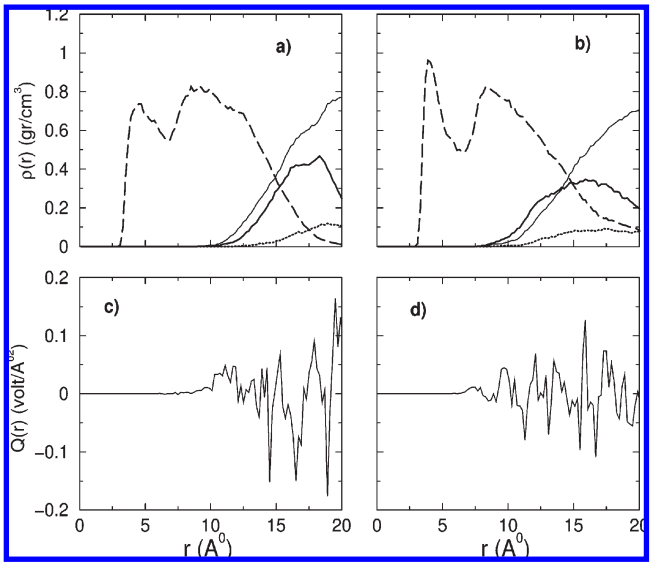

Figure 8. (a and b) *r*-density profiles [$\rho(r)$] for NaCl concentrations of 0.0166 and 0.0331 cc, respectively. (c and d) Total charge density profiles [$Q(r)$] for NaCl concentrations of 0.0166 and 0.0331 cc, respectively. The notation is the same as in Figure 5.

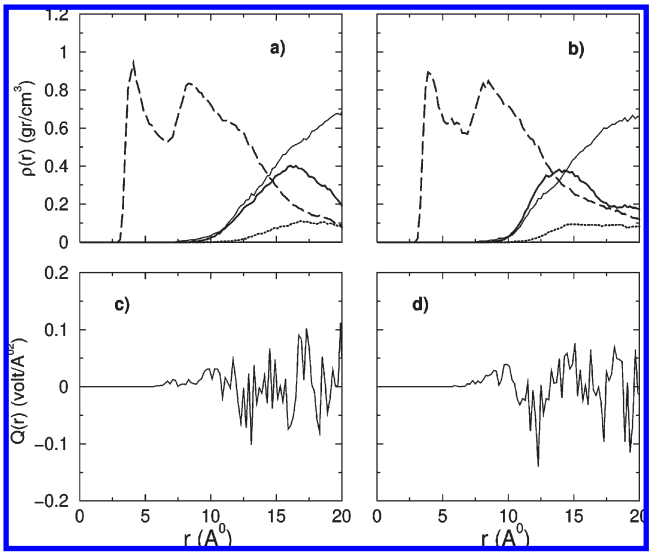

Figure 9. (a and b) *r*-density profiles [$\rho(r)$] for NaCl concentrations of 0.0497 and 0.0662 cc, respectively. (c and d) Total charge density profiles [$Q(r)$] for NaCl concentrations of 0.0497 and 0.0662 cc, respectively. The notation is the same as in Figure 5.

60 ± 3°, 59 ± 1°, 49 ± 2°, 48 ± 1°, and 35 ± 1° for NaCl concentrations of 0.0, 0.0166, 0.0331, 0.0497, and 0.0662 cc, respectively. The data are also given in Table 1. Despite the fact that some angles were similar (within the error bars), it was clear that the contact angle decreased as the salt concentration increased. Therefore, the results indicated that the SDS aggregates wet the surface more thoroughly as the salt concentration increased.

Moreover, from those calculations, I also concluded that the hemicylinders were not half-cylinders with radii of 17 Å [the height calculated from the $\rho(z)$ profiles]. The radii of the fitting circles (R), for all the concentrations, were different, indicating that the aggregates were only slices of cylinders which did not include the diameter of the enclosing circles.

3.2. Salt Concentration Effects. It is important to mention that the lowest concentration of salt represented a concentration of ~0.46 M; i.e., it was a solution much more concentrated than that used in experiments with the same systems (0.16 M NaCl).[21]

Because of the oxygens in the headgroups, the level of Na^+ ions close to those groups increased with the concentration as shown in Figures 4c, 5c,d, and 6c,d. In these figures, we observe a large number of Na^+ ions close to the headgroups and the numbers increase as the concentration increases, whereas the Cl^- ions were distributed more uniformly in the system (see Figures 4c, 5c,d, and 6c,d). Here, the ion profiles were multiplied by 10 for a better visualization. When the $\rho(r)$ profiles were analyzed, similar information was obtained. However, from those profiles (Figures 8 and 9), ions above the hemicylindrical structure and slightly farther from the headgroups were observed.

A quantity which is directly related to the ion concentration is the charge distribution in the system. Then, in Figures 4d, 8c,d, and 9c,d, charge density profiles (as a function of the radial distance of the hemicylinder) were calculated [$Q(r)$]. Although the profiles presented considerable variations in charge density (the tails were not charged), the $Q(r)$ for all concentrations started around $r \approx 10$ Å, except for the zero NaCl concentration which started around $r \approx 5$ Å.

Moreover, from the $Q(r)$ information, it was possible to obtain electrical potentials calculated from the following expression:

$$\Delta\phi = \phi(r_2) - \phi(r_1) = -\int_{r_1}^{r_2} \mathrm{d}r' E_r(r') \qquad (1)$$

where the electric field in cylindrical coordinates was calculated by

$$E_r(r) = \frac{1}{r\varepsilon_0}\int r' Q(r')\,\mathrm{d}r' \qquad (2)$$

The electrical potential difference was calculated with the interval $\Delta r = r_2 - r_1$, where $r_2 = 17.0$ (the high of the hemicylinder) and r_1 was the *r*-distance (15.5, 17.3, 15.9, 16.4, or 15.5 Å, obtained from the previous section). This Δr interval was chosen since the headgroups were thought to be located in a shell (over the hemicylinder) of this width.

The values for the potential were as follows: $\Delta\phi = -51 \pm 4$, -17 ± 6, -17.0 ± 4, -9 ± 2, and -37 ± 13 mV for NaCl concentrations of 0.0, 0.0166, 0.0331, 0.0497, and 0.0662 cc, respectively. The data are also given in Table 1. These values have the same order of magnitude as those found in experiments with SDS adsorbed on activated carbon (between -100 and -60 mV)[39] and in experiments of SDS bulk micelles as a function of salt (between -74 and -11 mV).[40]

From the results, it was observed that the absolute electrical potential decreased as the salt concentration increased (within the error bars), except for the concentration of 0.0662 cc. The same tendency was observed in experiments with SDS bulk micelles as a function of salt concentration.[40] It was not clear why the highest concentration did not follow the decreasing behavior; however, we tried to understand it by analyzing Figure 9b. From that figure, we observed that the headgroup profile (dark solid line) presented a different shape (at the end of the curve) with respect to the other figures. Although we were not sure about the nature of

(39) Gallardo-Moreno, A. M.; Gonzales-Garcia, C. M.; Gonzalez-Martin, M. L.; Bruque, J. M. *Colloids Surf., A* **2004**, *249*, 57.
(40) Mchedlov-Petrossyan, N. O.; Vodolaskaya, N. A.; Yakubovskaya, A. G.; Grigorovich, A. V.; Alekseeva, V. I.; Savvina, L. P. *J. Phys. Org. Chem.* **2007**, *20*, 332.

Table 1. *r*-Distances of the Hemicylinder, Contact Angles, and Electric Potential Differences Calculated from All the Aggregates at Different Salt Concentrations

[NaCl] (cc)	*r*-distance of the hemicylinder (Å)	contact angle θ (deg)	electric potential $\Delta\phi$ (mV)
0.0000	15.5 ± 1	60 ± 3	-51 ± 4
0.0166	17.3 ± 1	59 ± 1	-17 ± 6
0.0331	15.9 ± 1	49 ± 2	-17 ± 4
0.0497	16.4 ± 1	48 ± 1	-9 ± 2
0.0662	15.5 ± 1	35 ± 1	-37 ± 13

this form (it could be some fluctuation in the simulations), this distribution affected the calculation of the $Q(r)$ profile and certainly the calculation of the electrical potential.

By using the electric field relation (eq 2), it was possible to estimate the surface charge density (σ_s) with the equation $\sigma_s = E/\varepsilon_0$. The values that we obtained were 0.050, 0.047, 0.042, 0.020, and 0.35 C/m^2 for NaCl concentrations of 0.0, 0.0166, 0.0331, 0.0497, and 0.0662 cc, respectively. These values where smaller than those found in works of bulk SDS micelles (0.19 C/m^2);[38] however, those works were conducted without any salt, and the micelle structure was a sphere.

4. Conclusions

By using molecular dynamics, series of computer experiments for studying the adsorption of the SDS surfactant on a graphite surface at different NaCl salt concentrations were performed. In all cases, the SDS molecules aggregated in hemicylindrical slices with Na^+ ions surrounding the headgroups. On the other hand, it was observed that the hemicylinders were formed faster as the salt concentration increased. This effect can be understood, since it is known that the critical micelle concentration of charge surfactants is reduced by the presence of salt in solution.[41,42] Therefore, the formation of aggregates is promoted by the addition of salt to the system.

The main effect produced by an increment in salt concentration was given in terms of the internal structure of the hemicylinders. The first conclusion is that the molecules did not gather radially inside the cylinder. At all the NaCl concentrations (even in its absence), the SDS molecules were arrayed horizontally in two well-defined layers parallel to the graphite surface. Moreover, at low concentrations a third layer was also depicted.

Because of the hydrophobic substrate, the tail groups interacted primarily with the graphite plate through van der Waals forces. In fact, it has been suggested that epitaxy is responsible for the alkane chains adsorbing parallel to a graphite symmetry axis.[10,43] Therefore, the alkane chains were absorbed on the graphite surface by forming layers. Furthermore, if we consider the tails groups as a subphase of carbon atoms, the formation of contact layers is not surprised since adsorption studies of fluids on solid plates have shown the formation of layers in systems with Lennard-Jones interactions.[44]

As the NaCl concentration increased, the third layer lost its structure until it vanished at the highest salt concentrations. At the same time, as the NaCl concentration increased, the shape of the headgroups profiles became shaper. A possible explanation of this behavior is as follows. With an increase in the amount of salt in the system, the electrostatic interactions are more screened and the van der Waals interactions become more important. Therefore, the strength of the interaction between the SDS and the surface increases, and this promotes adsorption of the molecules on the surface as the contact angle calculations suggested.

At high salt concentrations, the contact angle value indicated that the aggregate wet more thoroughly the surface than at low concentrations by modifying the shape of the hemicylinder. Therefore, at low concentrations, the hemicylindrical shape (closer to a half-cylinder) could better accommodate the layers of the tails. As the concentration increases, the hemicylinder span more, over the $X-Y$ plane, breaking the layer structure at the top of the hemicylinder.

Finally, the excess of the positive Na^+ ions also weaken the repulsive interactions between the negatively charged headgroups, forcing the headgroups to accommodate each other more effectively. This could explain the more structured headgroup density profiles that we observed.

Acknowledgment. I acknowledge support from DGAPA-UNAM through Grant IN102207 and DGESCA-UNAM for the KanBalam supercomputer facilities. I am also grateful to Dr. M. Rivera for careful reading of the manuscript, and I thank all the reviewers for their valuable comments to improve the manuscript.

(41) Hayashi, S.; Ikeda, S. *J. Phys. Chem.* **1980**, *84*, 744.
(42) Hunter, R. J. *Foundations of Colloid Science*; Oxford University Press: Oxford, England, 1989.
(43) Yeo, Y. H.; Yackoboski, K.; McGonigal, G. C.; Thompson, D. *J. Vac. Sci. Technol., A* **1992**, *600*, 10.
(44) Dominguez, H.; Allen, M. P.; Evans, R. *Mol. Phys.* **1999**, *96*, 209.